JOURNAL OF CATALYSIS 49, 189–200 (1977)

Study of the Interaction of Aliphatic Alcohols with TiO_2

II. On the Mechanism of Alcohol Dehydration on Anatase

I. CARRIZOSA AND G. MUNUERA

Inorganic Chemistry Department, University of Seville, Seville, Spain

Received August 3, 1976; revised February 14, 1977

Adsorption of primary, secondary and tertiary aliphatic alcohols on TiO_2 (anatase) has been studied by volumetric and ir techniques. The results agree with the previously reported coordination model for alcohol adsorption on this oxide, and a relation has been established between the "irreversible adsorptions" and the respective dipole moments of the alcohols. The dehydration mechanism of the above alcohols was elucidated on the basis of both TPD kinetic parameters and the distribution of isomer olefins. A concerted β-E_2 elimination has been found with a Hoffmann/Saytzeff product ratio that places TiO_2 between acidic and basic catalysts (e.g., Al_2O_3 and ThO_2). *Cis/trans* selectivity ratios for the 2-olefins have been related to the unsaturation of the coordination sites at the surface. The application of Taft's relation to mechanistic studies is discussed from a critical point of view.

INTRODUCTION

Decomposition of the members of homologous series of alcohols has been widely used to ascertain the mechanisms of heterogeneously catalyzed reactions. In this sense, the dehydration of alcohols over oxide catalysts has been studied for both mechanistic and catalyst characterization purposes (*1–4*). In connection with this kind of study, the use of Taft linear free-energy relationships (LFER) has been extended to the field of heterogeneous catalysis, following the early works of Kraus and others (*5–8*), and has been used as a tool for mechanistic analysis.

However, most of this work has been carried out on Al_2O_3, though, recently, ThO_2 (*9*), ZrO_2 (*10*), and even alkaline-earth oxides (*11*) have been considered as typical basic catalysts in contrast with the acidic alumina surface. A concerted β-elimination reaction has been observed in most cases, while *trans* or *cis* elimination has been reported, depending on the acid–base character of the surfaces (*9, 12*).

Few studies have been carried out on the dehydration of alcohols on TiO_2 (*13*) in spite of the fact that this oxide has acid–base properties that are intermediate between those of Al_2O_3 and ThO_2. Dehydration of several aliphatic alcohols has been carried out on the well-characterized TiO_2 (anatase) surface described in previous work (*14*). The temperature-programmed decomposition (TPD) method has been used to determine the kinetic parameters for the decomposition of alcohols, due to the fact that, as shown in previous work (*15*), data obtained by this method agree with those directly measured for the catalytic process in a flow reactor under appropriate conditions.

EXPERIMENTAL

Materials. TiO_2 (anatase) was the same sample as used in Part I of this series (*15*),

ISSN 0021-9517

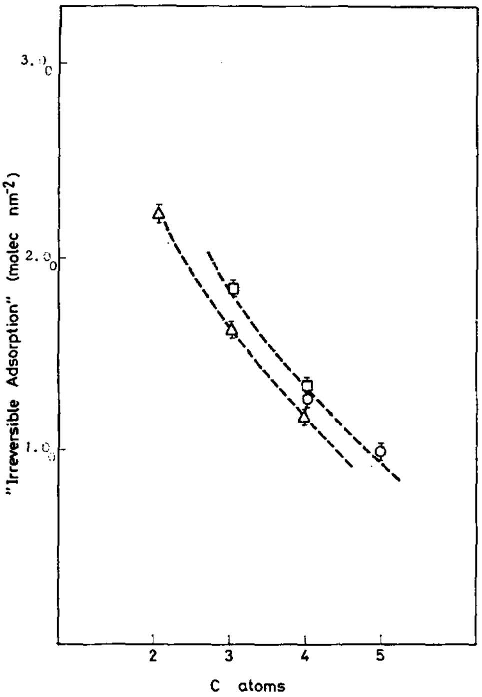

FIG. 1. "Irreversible adsorption" of aliphatic alcohols versus the number of carbon atoms: (△) primary, (□) secondary, (○) tertiary.

for which an atomic scale model of the surface had been developed (*14*) to explain its adsorption and catalytic properties.

Ethanol (EtOH), *n*-propanol (*n*-PrOH), *n*-butanol (*n*-BuOH), 2-propanol (2-PrOH), 2-butanol (2-BuOH), and t-butanol (t-BuOH) from Merck and t-pentanol (t-PeOH) from Fluka AG (all at least 99% pure) were redistilled on anhydrous $CuSO_4$ and were subjected to several freeze–pump–thaw cycles before using. Olefin used in gc identification were obtained by dehydration of the alcohols with P_2O_5.

Apparatus and procedures. Volumetric adsorption and infrared and TPD measurements were carried out following the same techniques and procedures described in our previous work (*15*). The kinetic parameters for the dehydration of the adsorbed alcohols were obtained from TPD data. The technique was similar to the auxothermic methods applied to the decomposition of solids in reactions of the type:

$$\text{A (solid)} \dashrightarrow \text{B (solid)} + \text{C (gas)},$$

so that the well-known shape index defined by Kissinger (*16*) was used to confirm the first-order character of the reactions.

RESULTS

Adsorption Isotherms and Infrared Studies

The "irreversible adsorption"capacity for each alcohol on the standard anatase surface (almost completely dehydroxylated), according to our previous definition (*15*), is shown in Fig. 1 plotted against the number of carbon atoms of the alcohol. The increase in alkyl chain length from C_2 to C_5 produces a progressive decrease in coverage. In the case of alcohols with the same number of carbon atoms, e.g., C_3 or C_4, the "irreversible adsorption" was only slightly different. However, secondary and tertiary alcohols were adsorbed in slightly larger amounts than were primary alcohols with the same number of carbons. This fact indicates that branching does not influence the adsorption capacity of the surface very much.

A detailed study of the adsorbed phase using ir spectroscopy for all primary alcohols and 2-PrOH and t-BuOH has been published elsewhere (*15*, *17*). The ir study of the remaining alcohols (2-BuOH and t-PeOH) supports behavior similar to that previously described for those alcohols. Both 2-BuOH and t-PeOH gave a "critical coverage" at 1 molecule nm^{-2}, as deduced from the plots of the corresponding ν_{OH} and ν_{CH} absorbances against the alcohol coverages. The intensity of the band at 3730 cm^{-1}, characteristic of the more basic surface hydroxyl groups, decreases with increasing coverages, while of the other two bands, the one at 3680 cm^{-1} increases more sharply, suggesting that the small dissociative adsorption occurring at room temperature, in equilibrium with the main molecular adsorption, should involve mainly the loss of alcoholic OH groups, as previously discussed for 2-PrOH and t-BuOH (*15*).

Thermal Decomposition of the Adsorbed Phase

Kinetic parameters (activation energies and frequency factors) for the dehydration of the adsorbed alcohols were obtained using the TPD method. This technique was previously shown to be a fast and powerful tool for kinetic studies of the decomposition of the adsorbed phase. Since the first-order character of the reaction has been well established both by ir and TPD in Part I of this series (*15*), it was only confirmed here by using Kissinger's shape index for the TPD peaks, included in Table 1.

Activation energies (E) and frequency factors (A) were obtained using several heating rates (β) and by applying the equation derived from the condition for the maximum in the TPD chromatogram:

$$2 \log T_M - \log \beta = E/2.3RT_M + \log E/AR.$$

As reported previously for EtOH, 2-PrOH, and t-BuOH, the alcohol was always adsorbed at room temperature on the standard treated surface until saturation, and then TPD scanning was carried out at several heating rates for each alcohol. The kinetic parameters obtained by the TPD method are summarized in Table 2.

TABLE 1

Shape Index and Reaction Order in TPD Dehydration of Alcohols Adsorbed on Anatase

Alcohol	Shape index (S)	Reaction order ($1.26\ S^{\frac{1}{2}}$)
EtOH	0.64	1.01
n-PrOH	0.57	0.96
n-BuOH	0.64	1.01
2-PrOH	0.60	0.98
2-BuOH	0.59	0.97
t-BuOH	0.62	0.99
t-PeOH	0.69	1.05

TABLE 2

TPD Kinetic Parameters for Dehydration of Alcohols Adsorbed on Anatase

Alcohol	Activation energy (kJ mol^{-1})	Frequency factor (s^{-1})
EtOH	76.5 ± 2	1.4×10^4
n-PrOH	89.0 ± 2	5.0×10^5
n-BuOH	91.9 ± 2	1.3×10^6
2-PrOH	92.0 ± 2	4.7×10^6
2-BuOH	62.7 ± 2	1.2×10^4
t-BuOH	54.3 ± 2	9.8×10^3
t-PeOH	37.2 ± 2	7.1×10^3

Activation energies increase with alkyl chain length in primary alcohols, while the opposite behavior was observed for secondary and tertiary alcohols. In comparing the C_4 alcohols, a decreasing activation energy can be observed when going from primary to tertiary species, in agreement with data reported for alumina (*4*). Moreover, a decrease in the temperature at which the olefin TPD-peak appears can be seen, following the pattern:

$$\text{Primary } (300°\text{C}) > \text{secondary } (250°\text{C}) > \text{tertiary } (200°\text{C}),$$

which suggests that removal of the alcoholic OH group, enhanced by the inductive effect of the alkyl chain, should be involved in the controlling step of the reaction for all three types of alcohol.

Evolution of the Olefins in TPD Experiments

In those cases in which several olefins could be formed, a detailed gc analysis of the evolved gases was carried out. In Fig. 2, analyses of pulses during the TPD scanning of 2-BuOH and t-PeOH are included, together with the TPD trace for each alcohol. The latter show a low-temperature shoulder derived, in both cases, from the desorption of some unreacted

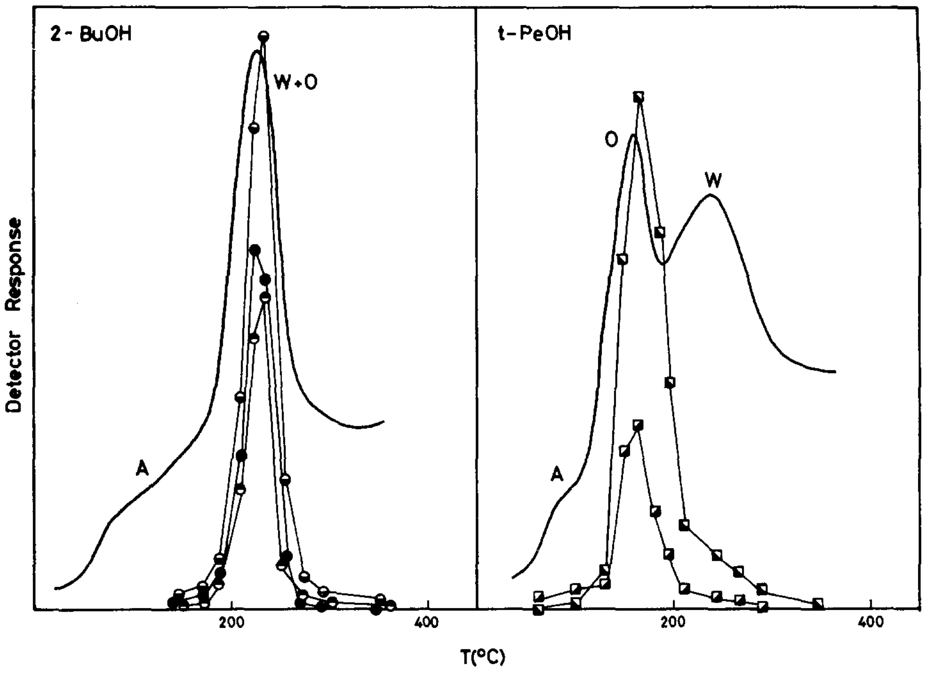

FIG. 2. TPD traces and gc analyses of pulses for 2-butanol and tert-pentanol (β = 8°C min^{-1}). A, alcohol; O, olefin; W, water. (●) 1-Butene; (◒) *cis*-2-butene; (◓) *trans*-2-butene; (◪) 2-methyl-1-butene; (◩) 2-methyl-2-butene.

alcohol adsorbed over ca. 1 molecule nm^{-2}. In the case of 2-BuOH, only one TPD peak is observed at 230°C due to simultaneous evolution of olefins and water, while, for t-PeOH, two maxima were well differentiated, one at 165°C due to the olefin mixture and the other at 250°C due to water. Thus, in this latter case, as shown previously with t-BuOH (*15*), water produced during alcohol dehydration is retained by the anatase surface and then desorbed at higher temperatures.

From gc analyses of the pulses it was found that dehydration of *n*-BuOH (the TPD trace of which is not shown) yielded 83% 1-butene and 17% 2-butenes (*cis* plus *trans*) during the entire TPD scanning, the *cis*/*trans* selectivity ratio being 2.9. These data suggest that decomposition occurs through an E_2 mechanism with only little participation from double-bond migration. In the case of 2-BuOH, which decomposes at lower temperatures than *n*-BuOH, the results were 16% of the Hofmann olefin (1-butene) and 84% of the Saytzeff products (2-butenes), with a *cis*/*trans* ratio of 3.5. The same analysis for t-PeOH gave a Saytzeff/Hofmann ratio (2-methyl-2-butene/2-methyl-1-butene) of 2.8.

Evolution of the isomer olefins throughout the TPD scanning can be followed in Fig. 3 in which the percentages of the respective olefins in the pulses were plotted against the sampling temperatures. For 2-BuOH, the olefin percentages were nearly constant up to 225°C (45% *cis*-2-butene, 32% 1-butene, and 23% *trans*-2-butene) and were far removed from the thermodynamic equilibrium values, which are represented in the same figure by dashed lines. Moreover, the percentage of *trans*-2-butene remains low and nearly constant throughout the entire TPD scanning, whereas, from 225°C, the *cis*-2-butene percentage readily increases, while the total amount of olefins becomes exhausted.

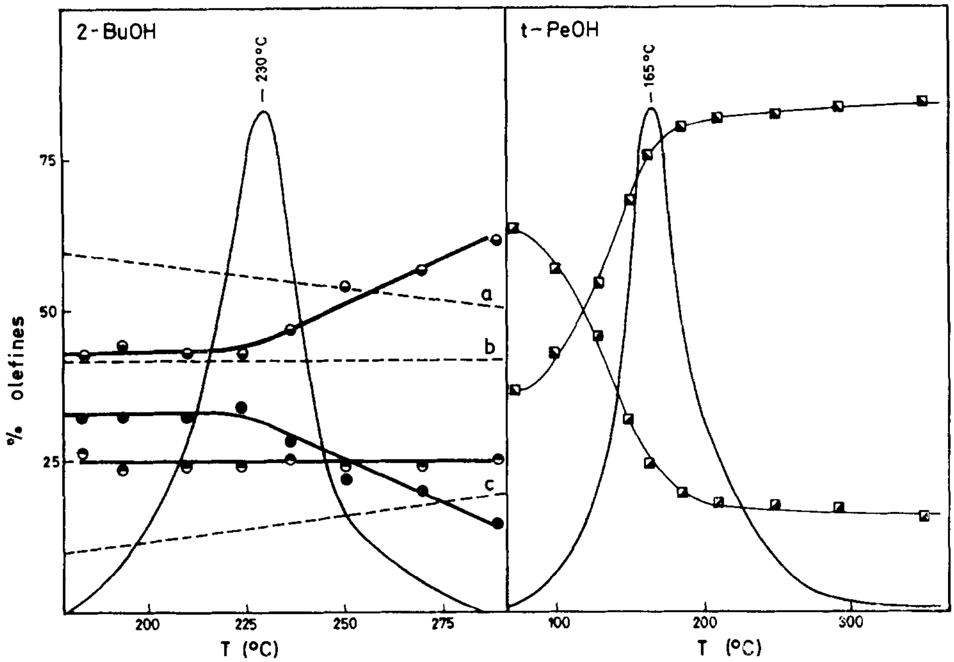

FIG. 3. Olefin TPD peak and isomer percentages for 2-butanol and t-pentanol dehydration. (●) 1-Butene; (◒) *cis*-2-butene; (◓) *trans*-2-butene; (◪) 2-methyl-1-butene; (◩) 2-methyl-2-butene. Dashed lines give equilibrium percentages for: (a) *trans*-2-butene; (b) *cis*-2-butene; (c) 1-butene.

For t-PeOH, Fig. 3 shows that, at the lower temperatures, the Hofmann product, 2-methyl-1-butene was also favored, but, on raising the temperature, the Saytzeff product, 2-methyl-2-butene, soon became the most important species. Furthermore, it is noteworthy that, in this case, at temperatures higher than 200°C, the percentage of 2-methyl-2-butene (ca. 80%) was higher than that corresponding to the thermodynamic equilibrium, ruling out a simple carbonium ion transition state (E_I mechanism) for this reaction.

DISCUSSION

Adsorption of aliphatic alcohols at room temperature on the standard dehydroxylated anatase surface (<2% OH coverage) used in this work yielded "irreversible adsorptions" which depended on the length of the alkyl chain and type of alcohol (namely, primary, secondary, or tertiary). However, as previously discussed (*15*), ir and TPD techniques discriminate between two types of adsorbed molecules: These are tightly adsorbed species that gives maximum coverages of ca. 1 molecule nm^{-2} for all the alcohols and a "residual adsorption" up to the experimentally measured "irreversible adsorption" coverages given in Fig. 1. Differences in saturation coverages have been ascribed to the influence of inductive and/or steric factors, or both, in determining the maximum coordination state that can be attained by the surface Ti^{IV} ions, as a consequence of the electroneutrality principle and/or steric hindrance produced by the alcohol ligands, similar to the situation reported by Bradley (*18*) for the respective alkoxides.

As supported by volumetric and ir data, the alcohol molecules should be adsorbed mostly in a nondissociative way, acting as bridging ligands between pairs of Ti^{IV} ions in a fourfold coordination at the surface, until they attain a fivefold coordination as previously discussed (*15*). The "residual adsorption" must now complete the sixfold coordination of some of these cations:

SCHEME I

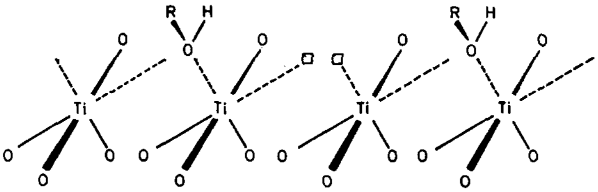

In the case of EtOH, all the cations attain this latter coordination, as occurs in the corresponding $Ti(OEt)_4$ alkoxide, the new molecules up to 2 EtOH nm^{-2} being accommodated on the remaining free coordination sites between Ti^{IV} pairs. However, even in this case, 50% of the adsorbed alcohol molecules are easily removed under mild thermal conditions. Further adsorption, in excess of 2 EtOH nm^{-2}, must now occur, involving O^{2-} and OH^- groups as suggested by changes in the ir spectra of the hydroxyl stretching region.

The amount of alcohol molecules in excess of 1 *R*OH nm^{-2} suggests an electrostatic interaction with the surface, as indicated by the observed relationship between the maximum "irreversible adsorption" for *n*-alcohols and the respective dipole moments of these alcohols in Table 3. The same sequence seems to hold for secondary and tertiary alcohols (e.g., *n*-PrOH against 2-PrOH or *n*-BuOH against t-BuOH), though steric effects may also contribute to the actual values of the coverages.

Assuming the twofold interaction previously proposed (*15*), both alcoholic oxygen and hydrogen should be involved in the interaction with a "Ti-O" site (H bonding leading to the ir band at 3480 cm^{-1}). Indeed, a better way to quantify this interaction would be to use the dipolar components due to the OH group in the alcohols, but, unfortunately, these are unknown.

The importance of the dipolar component due to the OH group of the alcohol in the interaction process with the surface is further supported by the fact that the adsorption of *n*-chlorobutane on the same anatase sample gives a Type III BET isotherm, indicating a very weak interaction with the surface, in spite of the higher dipole moment of this molecule (*19*).

As previously reported (*15*), residual surface hydroxyl groups (2% full coverage) are only weakly involved in the interaction of the tightly adsorbed molecules; nevertheless, ir spectra show that, at room temperature, a small number of the alcohol molecules are adsorbed in a dissociative way, increasing the intensity of the free hydroxyl bands at 3680 and 3620 cm^{-1}. The change of intensity of these bands

TABLE 3

"Irreversible Adsorption" of Alcohols on Anatase Standard Treated Surface and Dipole Moments of the Alcohols

	HOH[a]	EtOH	*n*-PrOH	*n*-BuOH	2-PrOH	t-BuOH
Adsorbed amount (molecules nm^{-2})	3.06	2.25	1.63	1.20	1.85	1.35
Dipole moment (Debye units)	1.81	1.69	1.64	1.63	1.68	1.66

[a] Water is included for comparative purposes.

after adsorption of 2-BuOH and t-PeOH supports a dissociative adsorption with detachment of the OH alcoholic group, leaving the alkyl group free to react with the most basic O^{2-} ions at the surface.

When the temperature is raised, weakly adsorbed molecules (in excess of 1 molecule nm^{-2}) desorb, while a fraction of the more tightly adsorbed molecules dissociates to form alcoholate species. In addition, adsorbed molecules and/or alcoholate species should be able to jump from one coordination site to another, producing a certain "fluxionality" of the adsorption complex that should behave in a way rather similar to fluxional ligands in polynuclear coordination compounds, as has been suggested by Ugo (*20*). Coordinative unsaturation of the Ti^{IV} ions must facilitate this movement so that it seems very likely that the adsorbed phase, formed by alcohol and alcoholate species, changes from a primarily immobile adsorption complex at room temperature to a mobile one when the temperature rises just before decomposition starts.

Dehydration Mechanism

For the alcohols studied in this work, the possibility of a β-elimination mechanism to yield olefin and water always exists, since H_β is present in all of them. This reaction is favored at the antase surface, where the low acidity of the exposed Ti^{IV} ions seems to preclude the formation of strongly covalent bonded alcoholates which, according to Knözinger (*3*), are responsible for ether formation on alumina through a bimolecular process. In fact, traces of ether were observed only in the TPD experiments in the case of ethanol, at temperatures slightly higher than those of olefin evolution.

On anatase surfaces, dehydration to olefins involves Ti^{IV} sites assisted by O^{2-} or OH^- ligands in the coordination sphere of the metal ion, as has been previously discussed (*15*). This site is different from that originally described by Knözinger *et al.* for alumina (*4*), on which adsorption is assumed to occur via Brønsted OH groups, on the basis of the lack of poisoning of the reaction by pyridine. However, these poisoning experiments do not, in our opinion, invalidate Lewis sites as active centers for the reaction, even on alumina, since pyridine is tightly adsorbed only on strongly acidic Lewis sites (those involved in ether formation), rendering the less acidic ones available for monomolecular dehydration of the alcohols to olefins.

Concerted E_2 mechanisms have been widely invoked for monomolecular dehydration of alcohols on metal oxides. Our results on temperature-programmed decomposition of adsorbed alcohols on TiO_2 (anatase) support this kind of mechanism as well, with only small ionic deviations toward E_1 or E1cB transition states, depending on the inductive and/or steric effects of the alkyl groups linked to the C_α and the C_β atoms. Thus, the product distribution upon TPD dehydration of *n*-butanol, 1-butene/2-butenes = 4.2, indicates an almost entire lack of isomerization of the primary product, 1-butene, during TPD scanning, while the values given in Fig. 3 for 2-butanol and tert-pentanol support an E_2 mechanism, because, in both alcohols, the percentages of the isomer olefins were far removed from the thermodynamic equilibrium which would be attained in all the cases if an E_1 mechanism via carbonium ions was acting.

In the case of primary alcohols, the inductive effect of the alkyl chain linked to the C_β atom should have a double effect on the removal of the OH_α and H_β atoms:

SCHEME II

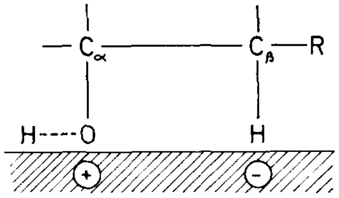

First, the inductive effect of the *R* group increases the electron density at the OH group, thus favoring a strong interaction of this group with the Ti^{IV} site at the surface and its detachment as a charged ion from the alcohol. On the other hand, the electron density would also increase on the C_β atom, thus making the elimination of the H_β as a proton by an O^{2-} ligand more difficult. The two synergic effects preclude the prediction of any trend for changes in the activation energy with the nature of the alkyl radical. Thus, the observed sequence for these primary alcohols (Table 2), rising from EtOH to *n*-BuOH, suggests that the second effect overcomes the first one on anatase, leading to a small displacement from an E_2 toward an ElcB-like mechanism.

The changes in the activation energies for the secondary and tertiary alcohols studied in this work can also be understood on the basis of a concerted E_2 mechanism, when inductive effects of the alkyl groups linked to the C_α and the C_β atoms are taken into account. The following scheme shows the structural relations between the four alcohols, and the activation energies referred to the Hofmann dehydration product, which appears at lower temperatures when the kinetic control of the reaction is more important:

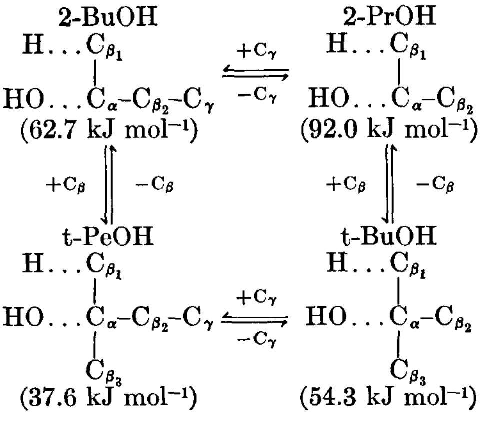

The high preference for the Hofmann products at the lower temperatures during dehydration of 2-BuOH and t-PeOH can be ascribed to the inductive effects of the γ-CH_3 group in lowering the acidity of the H_{β_2} protons directly bonded to the methylene C_{β_2} atom. The sequence of activation energies, decreasing when the inductive effect of the alkyl chain on the C_α atom increases, suggests that, for these molecules, the change in the lability for elimination of the OH group is the main factor determining the activation energy of the whole process, provided that the H_{β_1} elimination to give the Hofmann olefin (1-butene or 2-methyl-1-butene) remains almost unaffected by the substituents on the C_{β_2} atom. These facts suggest a displacement of the E_2 mechanism toward an E_1-like one as the chain length linked to the C_α atom increases.

The noticeable tendency of the anatase surface to form Hofmann olefin allows us to classify this surface as being intermediate between Al_2O_3, with a high Saytzeff preference (*12*), and ThO_2 (*9*) or ZrO_2 (*10*) with a Hofmann preference. Since the product distribution of 1-BuOH, 2-BuOH, and t-PeOH is far removed from thermal equilibrium at each temperature and, in the latter alcohol, is in excess of the equilibrium value even at higher temperatures, we may conclude that, in all cases, an E_2 mechanism is operative during TPD measurements. Several authors have confirmed (*12*, *21*) a *trans*-E_2 elimination of the OH_α and H_β groups on alumina to give the Saytzeff olefin, while Lundeen and van Hoozer (*9*) have shown that the reaction proceeds giving the Hofmann olefin on ThO_2 via a *cis*-E_2 elimination mechanism. Both *trans*- and *cis*-E_2 elimination may occur simultaneously on our anatase sample in a ratio that depends on the temperature, a situation similar to that recently found by Thomke and Noller (*22*) for dehydration of 2-BuOH on alkaline-earth orthophosphates.

The possibility of both a *trans*- and *cis*-E_2 elimination and the influence of steric effects on the *cis*/*trans* selectivity ratio suggest that the symmetry and the coordination state of the sites at the surface are of paramount importance in the course of the reaction, as was previously assumed by Knözinger *et al.* in the case of alumina catalysts (*4*).

Taking into account the adsorption model for the alcohols discussed in a previous paper (*15*), adsorption of 2-BuOH must occur at room temperature with the CH_3 group oriented with preference toward the most exposed O^{2-} ions at the surface [labeled 1 in Fig. 7 of Ref. (*15*)], while the bulky CH_3–CH_2 group will become directed outside the surface, as shown in scheme III(a) below.

SCHEME III

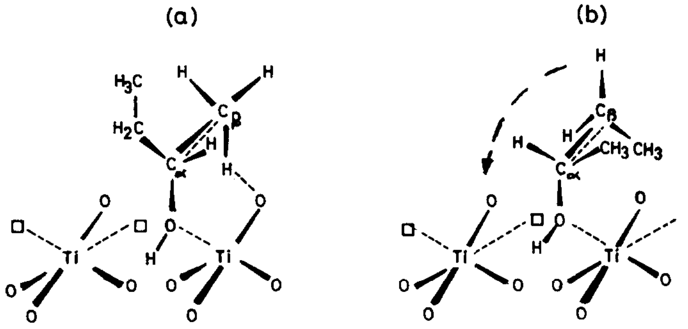

Cis-elimination
1-butene
(Hofmann product)

Trans-elimination
cis-2-butene
(Saytzeff product)

This arrangement should facilitate the elimination of a proton from the CH_3 group by the highly basic O^{2-} ion from a *cis* position relative to the oxygen atom of the alcoholic OH group, thus favoring the formation of 1-butene. During the TPD scanning process, the possibility of rotation and/or jumping of the alcohol ligand on the surface coordination sites when the temperature rises should become enhanced. A simple rotation of 180° of the alcohol molecule around its C–O bond on the adsorption site will bring the CH_3–CH_2 group close to the basic O^{2-} ions, promoting the formation of 2-olefin in the same active centers. However, as deduced from the data in Fig. 5, the centers giving the 1-olefin are able to give only the *cis*-2-olefin from 2-butanol, now that the *trans*-2-olefin percentage remains unchanged throughout the entire TPD scanning process. This fact, together with the high *cis/trans* ratio, could be explained by assuming a transition-state model similar to that previously proposed by Knözinger *et al.* (*4*) for alumina catalysts, though involving, in our case, a coordinative interaction of alcohol molecules with Ti^{IV} ions at the anatase surface [instead of the OH-bonded species assumed by Knözinger *et al.* (*4*)]. According to this model, the alcohol molecule should retain some vibrational and rotational freedom relative to the surface in the decomposition site. This enables the H_β in an anti-periplanar position relative to the OH alcoholic group to approach a basic surface site, which, in our case, should be one of the basic and highly exposed O^{2-} ions in the neighborhood of the coordination site (Ti^{IV} ion). The existence of these prominent basic oxygen sites may facilitate the abstraction of H_β from the methylenic group

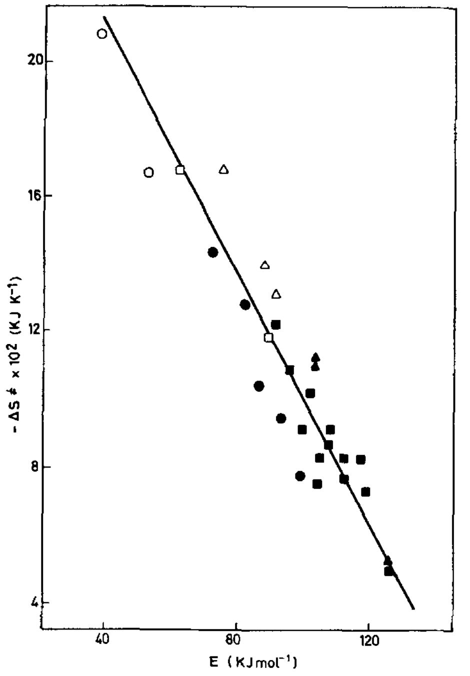

FIG. 4. Compensation effect for dehydration of aliphatic alcohols on anatase and alumina. (△▲) Primary alcohols on anatase and alumina; (□■) secondary alcohols; (○●) tertiary alcohols.

in the anti-periplanar position via an inclination movement (wagging of the molecule) of the plane where the preformed olefin transition state is contained. This kind of movement, as pointed out by Knözinger *et al.* (*4*) would be favored only if the bulky substituents in C_α and C_β are in the synclinal position and on the opposite side of the basic center, as shown in scheme III (b) above, thereby producing exclusively the *cis* isomer. In fact, Fig. 3 shows that, at $t > 225°C$, the amount of *cis*-2-butene readily increases at the cost of 1-butene, supporting the same active sites in the formation of both olefins. On the other hand, the small percentage of *trans*-2-butene (as compared with the equilibrium values), almost constant throughout the TPD scanning, suggests that this olefin should be produced at a different type of site, probably related to poorly coordinated Ti^{IV} ions in which steric hindrance does not play an important role and, thus, favoring a *cis* elimination of the alcoholic OH_α and H_β. The number of this kind of center seems to be small, thus determining the distribution of the 2-olefins throughout the TPD experiments.

Linear Free-Energy Relationships

The kinetic parameters in Table 2 show the existence of a compensation effect between activation energies and frequency factors. A similar correlation has been reported by Lane *et al.* (*23*) for the same reaction on Al_2O_3. Data from Knözinger *et al.* (*4*) on the same oxide fit in with our own results as shown in Fig. 4, while the data of Lane *et al.* gave a parallel straight line. As can be seen in this figure, the compensation effect seems to be slightly different for the three types of alcohol, data for primary and tertiary alcohols being displaced, respectively, downward and upward of the line containing the secondary ones, thus confirming the small differences between the three series of aliphatic alcohols observed on adsorption.

The low frequency factors observed in Table 2 should be ascribed, as discussed in Part I (*15*), to negative adsorption entropies for the decomposition of the alcohols. Our previous view of a mobile adsorbed phase under precatalytic conditions supports these values if decomposition occurs when one adsorbed molecule reaches a Ti^{IV} site where it becomes tightly bonded and gives rise to the above described transition states with restricted mobility. In this way, the reaction could be described as a bimolecular process between the mobile adsorbed phase and a certain number of sites on which decomposition occurs. The coincidence in the compensation effect of data for TiO_2 in this paper with the results for Al_2O_3 (*4*) suggests that the nature and number of such sites should be rather similar in both oxides, while the small parallel displacement of the data of Lane *et al.* (*23*) can

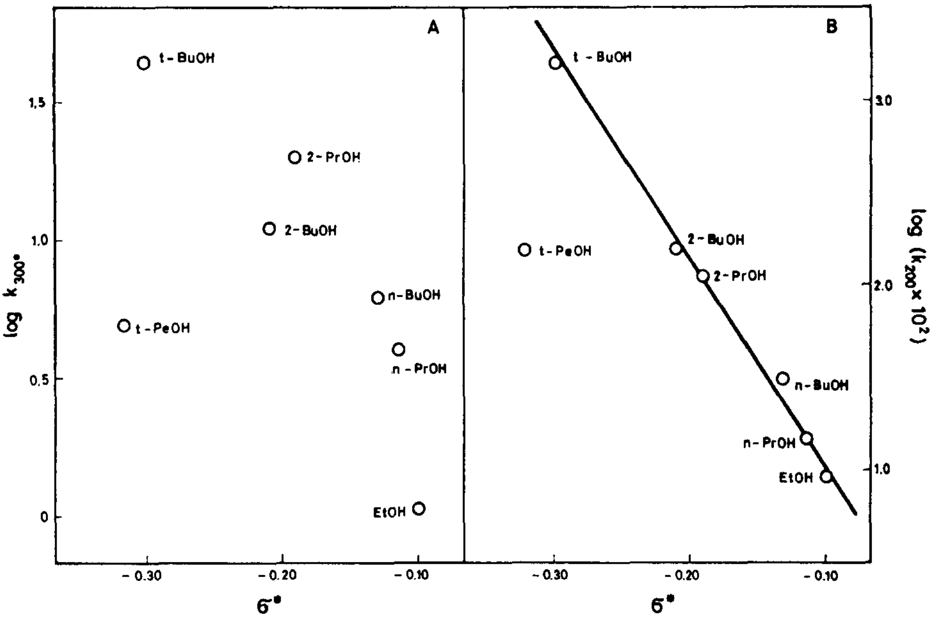

FIG. 5. Taft representation for aliphatic alcohol dehydration at (A) 300 and (B) 200°C.

be ascribed to a lower number of active sites in their samples.

Besides these compensation effects, correlations between the rate constant at a given temperature and Taft's inductive and steric parameters, σ^* and E^*_s, have been widely used in order to explain the mechanisms of heterogeneously catalyzed elimination reactions. In Fig. 5, rate constants at 200°C (k_{200}), deduced from the data in Table 2, have been plotted against the σ^* values for the alkyl chain attached to the alcoholic OH group, as was previously done by several authors (*3–6*). A good correlation was obtained in spite of the deviation of the value for t-PeOH, which can be ascribed to steric effects for this highly branched alcohol (*24*). From this plot, a value of $\rho^* = -10.7$ is found, suggesting a highly ionic transition state during the dehydration process. However, this latter conclusion does not agree with the previously assumed E_2 mechanism and moreover, the rate constants at 300°C (k_{300}), also shown in Fig. 5, do not follow any correlation at all, showing that our former Taft correlation was fortuitous and, therefore, not meaningful. Results similar to those shown in Fig. 5 could be obtained using the sum of the σ^* values of the groups linked to the C_α atom as the correlation parameter, as used by Kibby and Hall (*24*), though the selection of the σ^* parameter in both cases was incorrect in a strict sense, as pointed out by Criado (*25*).

Several further points should be stressed in connection with the use of Taft correlations for mechanistic studies in the field of heterogeneous catalysis. Criado (*25*) has shown that the value of ρ^* depends on the temperature, and, therefore, changes in the ρ^* value can be expected without any change of mechanism, thus putting into considerable doubt mechanistic conclusions obtained from relative values and sign changes of this parameter. Conclusions based upon such correlations in heterogeneously catalyzed reactions should be used very cautiously, and more detailed work must be done to establish a bridge between these correlations, when properly used, and the surface properties of the catalyst.

REFERENCES

1. Heiba, E. A., and Landis, P. S., *J. Catal.* **3**, 471 (1964).
2. Stauffer, J. E., and Kranich, W. L., *Ind. Eng. Chem. Fundam.* **1**, 107 (1962).
3. Knözinger, H., *Angew. Chem. Int. Ed. Engl.* **7**, 791 (1968).
4. Knözinger, H., Buhl, H., and Kochloefl, K., *J. Catal.* **24**, 57 (1972).
5. Kraus, M., *in* "Advances in Catalysis" (D. D. Eley, H. Pines, and P. B. Weisz, Eds.), Vol. 17, p. 75. Academic Press, New York, 1966.
6. Lopez, F. J., Andréu, P., Blassini, O., Paez, M., and Noller, H., *J. Catal.* **18**, 233 (1970).
7. Kochloefl, K., Kraus, M., and Bazant, V., *in* "Proceedings, 4th International Congress on Catalysis, Moscow, 1968." Paper 85, 1968.
8. Kochloefl, K., and Knözinger, H., *in* "Proceedings, 5th International Congress on Catalysis" (J. Hightower, Ed.), Vol. 2, p. 1171. North-Holland, Amsterdam, 1973.
9. Lundeen, A. J., and Van Hoozer, W. R., *J. Org. Chem.* **32**, 3386 (1967).
10. Yamaguchi, T., Sasaki, H., and Tanabe, K., *Chem. Lett.* 1017 (1973).
11. Krylov, O. V., Markova, Z. A., Tretyakov, I. I., and Fokina, E. A., *Kinet. Katal.* **6**, 128 (1965).
12. Hall, W. L., *Diss. Abstr.* **B27**, 754 (1956).
13. Knözinger, H., *in* "The Chemistry of the Hydroxyl Group" (S. Patai, Ed.), p. 641. Interscience, New York, 1971.
14. Munuera, G., Moreno, F., and Gonzalez, F., *in* "Proceedings, 7th International Symposium on Reactivity of Solids," p. 681. Chapman and Hall, London, 1973.
15. Carrizosa, I., and Munuera, G., *J. Catal.* **49**, 174–188.
16. Kissinger, H. E., *Anal. Chem.* **29**, 1702 (1957).
17. Carrizosa, I., and Munuera, G., *in* "Proceedings, 3rd Iberoamerican Symposium on Catalysis." *Acta Cient. Venezol.* **24**, 226 (1973).
18. Bradley, D. C., *in* "Progress in Inorganic Chemistry" (F. A. Cotton, Ed.), Vol. 2, p. 303. Interscience, New York, 1960.
19. Munuera, G., unpublished results.
20. Ugo, R., *Catal. Rev.* **11**, 225 (1965).
21. Pines, H., and Manassen, J., *in* "Advances in Catalysis" (D. D. Eley, H. Pines, and P. B. Weisz, Eds.), Vol. 16, p. 49. Academic Press, New York, 1966.
22. Thomke, K., and Noller, H., *in* "Proceedings, 5th International Congress on Catalysis" (J. Hightower, Ed.) Vol. 2, p. 1183. North-Holland, Amsterdam, 1973.
23. Lane, R. M., Lane, B. C., and Phillips, C. S., *J. Catal.* **18**, 281 (1970).
24. Kibby, C. L., and Hall, W. K., *J. Catal.* **29**, 144 (1973).
25. Criado, J. M., *in* "Proceedings, 4th Iberoamerican Symposium on Catalysis," Mexico D. F., 1974, in press.